

Extended Abstract for ASPEN2022

A large-scale nanomachining system established based on AFM contact mode

Jiqiang Wang¹, Yanquan Geng¹, Junshuai Jia¹ and Yongda Yan^{1,#}

¹ Center for Precision Engineering, Harbin Institute of Technology, Harbin, Heilongjiang 150001, P.R. China
Corresponding Author / Email: yanyongda@hit.edu.cn, TEL: +86-0451-86412924, FAX: +86-0451-86412924

KEYWORDS: Large-scale nanomachining, Contact mode, Variable force control machining

As a new nanomachining technology, atomic force microscope (AFM) tip-based nanomachining technique has the merits of easy processing, low equipment cost, low requirement on the machining environment as well as nanometric machining precision. Moreover, nanostructures with a constant depth can be machined on inclined surfaces, curved surfaces and even complex surfaces with the aid of the constant force machining characteristics. However, most of the present AFM tip-based nanomachining process are carried out on a commercial AFM system, which is limited by the small working range and normal force. To overcome these limitations, a homemade micro/nano machining device is developed in this study based on the contact mode of the AFM system. The maximum machining range and normal load are increased to 50 mm and 100 μN , respectively. The large-scale machining process is achieved based on two high-precision stages driven by air floatation. To realize the motion control of the platform, real-time acquisition of signals and the setting of PID controller parameters, the hardware and software system of the device are developed. The stability of the PSD signal under open-loop situation is measured to eliminate the factors that affects the system stability as far as possible. The steady and dynamic performance of the control system are evaluated by measuring the output response curve of the control system under step input. The output responses of the control system under triangular wave and sinusoidal wave signals with different frequencies are observed to verify the feasibility of variable force control machining. The machining subroutines are established to achieve the self-defined trajectory machining and variable force control machining. Nanoripple structures with controllable period are fabricated based on the variable force control method. Furthermore, the influence of processing parameters on the machining outcomes is analyzed. A large-scale micro/nano structure machining experiment is carried out and the machining quality of the obtained structures is evaluated.

1. Introduction

Nanostructures can be used in fields of optical [1], surface enhanced Raman scattering [2] and bionic [3]. Thus, fabrication of nanostructure has drawn great attention in the past few years.

Several micro and nanofabrication techniques, such as photolithography [4], nanoimprinting [5], electron beam lithography [6] and focused ion beam lithography [7], are utilized to fabricate nanostructures. However, these methods are limited by some disadvantages. For instances, the resolution of photolithography is limited by the wavelength and the preparation process requires a long time. For the nanoimprinting technique, fabrication of the template with a high-precision is difficult. The high-energy beam machining techniques (FIB and EBL) are difficult to machine a large-scale nanostructure and the investment for the facility is extremely high.

Atomic force microscope (AFM) tip-based nanomachining technique has been proven as a facilitating tool to fabricate nanostructures [8]. Nanoripples and nanodots are prepared on polycarbonate (PC) sheet by using a commercial AFM system [2]. However, the machined area of these nanostructures is less than 100 $\mu\text{m} \times 100 \mu\text{m}$ owing to the limiting of the travel range of the PZT tube. Thus, how to fabricate a large-scale nanostructure (up to mm) with high machining efficiency is still a challenge.

In this study, a homemade micro/nano machining device is developed based on the contact mode of the AFM system. The maximum machining range are increased to 50 mm. Furthermore, the maximum normal load is 100 μN . The steady and dynamic performance of the control system are evaluated. A large-scale nano-grid is machined based on the proposed machining device.

2. The homemade large-scale micro/nano machining device

The proposed large-scale nanomachining device works with the sample scan mode. Fig. 1(a) illustrates the schematic diagram of the device, which is mainly composed of the force sensor system, 3D piezoelectric positioning stage and 2D large scale precision positioning platform. The force-sensing system are used to achieve the micro-force control machining. As shown in Fig. 1(b), it is made up of a laser, PSD, optic lens and tip holder. The course movement of the tip is based on the Z-stepper motor. The manual stage is used to adjust the laser angle, which guarantees the laser illuminated on the ideal position of the probe cantilever. The reflector adjustment frame is used to adjust the propagation direction of the reflected light path, so that the light spot is irradiated on the expected position on the PSD. A CCD is fixed horizontally below the force sensing system. Thus, the laser alignment of the probe cantilever and the surface of the sample could be observed through it. The 3D piezoelectric positioning stage is fixed on the 2D large scale precision positioning platform, which is used to control the micro-motion of the sample, and at the same time, it forms a force closed-loop control system with the force sensing system. The large-scale machining is achieved on the movement of the 2D large scale precision positioning platform. The whole device is fixed on a vibration isolation platform to impede the outside vibration.

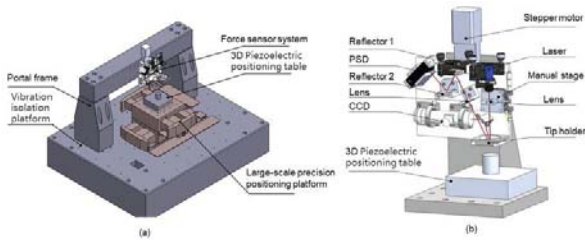


Fig. 1 (a) Schematic diagram of the large-scale nanomachining device. (b) Force-sensing system.

Fig. 2 shows the diagram of the control system. The host computer controls multi-function I/O device by calling the dynamic link library function. The control of the relative displacement and speed of the Z-stepper motor is achieved by sending pulse signal to the stepper motor through the pulse signal output port of the multi-function I/O device. Real-time acquisition of X_{diff} , Y_{diff} , Sum voltage signals of PSD and X, Y, and Z axis position voltage signals of the PZT is realized through the analog input port of the multi-function I/O device, The collected signals are displayed in the host computer. An analog voltage of 0~10V can be applied to the X and Y axes of the piezoelectric positioning stage through the analog output port of the multi-function I/O device to realize the movement of the scanning track or the custom track.

The control system realizes the closed-loop control of the analog quantity through the PID controller. The parameters and working mode of the PID controller can be set by the host computer through the serial port command. The Y_{diff} voltage signal of the PSD inputs to the

Measure port of the PID controller as a feedback signal. The output voltage of the PID controller controls the motion of the Z-axis of the 3D piezoelectric positioning stage. Hence, a complete closed-loop loop with the force sensing system is achieved.

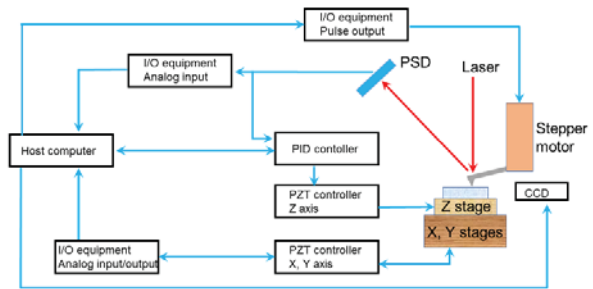


Fig. 2 The diagram of the control system.

3. Results and discussion

3.1 Response speed evaluation of closed-loop control system

To evaluate the response speed of the closed-loop control system, the output of the close-loop control system is investigated. Different sinusoidal wave signals generated from a signal generator are inputted to the PID controller. Meantime, the input signal and the output are recorded. Fig. 3 shows the output response of the system relative to different frequency sinusoidal waves. As shown in Fig. 3(a), the output signal follows the input signal with almost no delay when the frequency is 8 Hz. Fig. 3(b) illustrates the output response when the frequency is 2000 Hz. It is observable that the delay is less than 2 ms. This indicates the variable force-controlled machining can be achieved on this system.

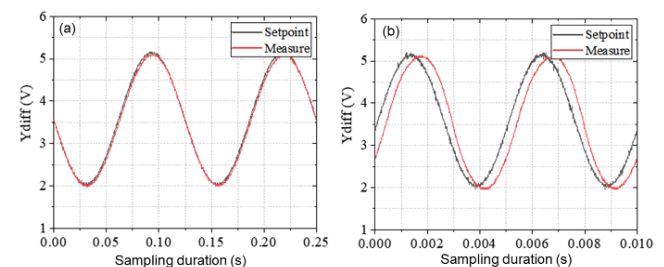


Fig. 3 Output response of the closed-loop control system relative to different frequency sinusoidal wave. (a) 8 Hz, (b) 2000 Hz.

3.2 Nanostructure fabrication

To verify the machining ability of the established device, four designed nanostructures are fabricated in this section. Figs. 4(a), (b), (c) and (d) show the rectangular, triangular, circle and cross-shape arrays machined on a PC sheet. One can see that the machined nanostructures have a good consistency. There is almost no scratching trace on the adjacent of the nanostructures. This indicates the established devices can be used to machine nanostructures.

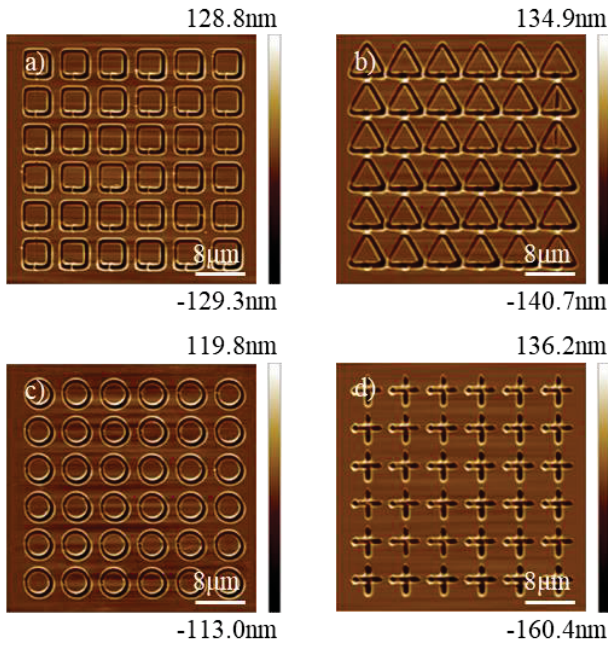


Fig. 4 Nanostructure arrays. (a) rectangular, (b) triangle, (c) circle, (d) cross-shape.

The variable force-controlled nanomachining is performed to fabricate nanoripple structures. Fig. 5(a) shows the schematic diagram of the applied variable force. The period and machined range are termed as T and W , respectively. The max and min represent the maximum and minimum applied normal force. Fig. 5(b) illustrates the schematic of the tip trace for fabricating nanoripple. The machining range is $W \times W$. The feed value is indicated as D . In the nanomachining process, the tip scratches along the fast-scan axis and feed with the slow-scan axis direction. Figs. 5 (c) and (d) demonstrate the AFM image and corresponding cross-section of the machined nanoripple. The minimum and maximum normal forces used to machine this nanoripple are $8.29 \mu\text{N}$ and $58.02 \mu\text{N}$, respectively. Furthermore, the machining velocity is $30 \mu\text{m/s}$. It is obvious the nanoripple has a good period. Moreover, the period of the nanoripple is consistent with the period of the applied normal force.

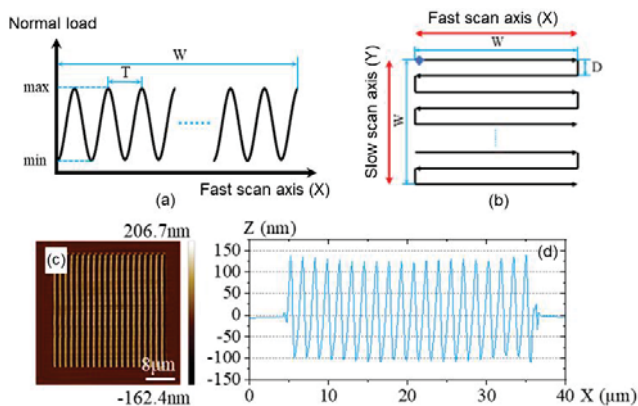


Fig. 5 Schematic diagrams of the (a) applied variable force and (b) the tip trace. (c) The AFM image and (d) corresponding cross-section of

the machined nanoripple.

3.3 Large-scale nano-grid fabrication

As shown in Fig. 6, a large-scale nano-grit ($0.9 \text{ mm} \times 0.9 \text{ mm}$) is fabricated in this section. The distance between the adjacent scratching traces is 0.1 mm . The normal load and feed velocity are $12.57 \mu\text{N}$ and $100 \mu\text{m/s}$, respectively. To investigate the machining quality and positioning accuracy of the proposed device, eight areas of the nano-grit (indicated by 1, 2, 3, 4, 5, 6, 7 and 8 in Fig. 6) are measured by using commercial AFM. It is observable that the machined depths in areas 2, 3, 6 and 7 are identical. Furthermore, the intersection points (indicated by 1, 4, 5, and 8 in Fig. 6) show that the horizontal groove crashes on the vertical groove accurately, which indicates the proposed machining device has a good positioning accuracy and can be used to machine a large-scale nanostructure.

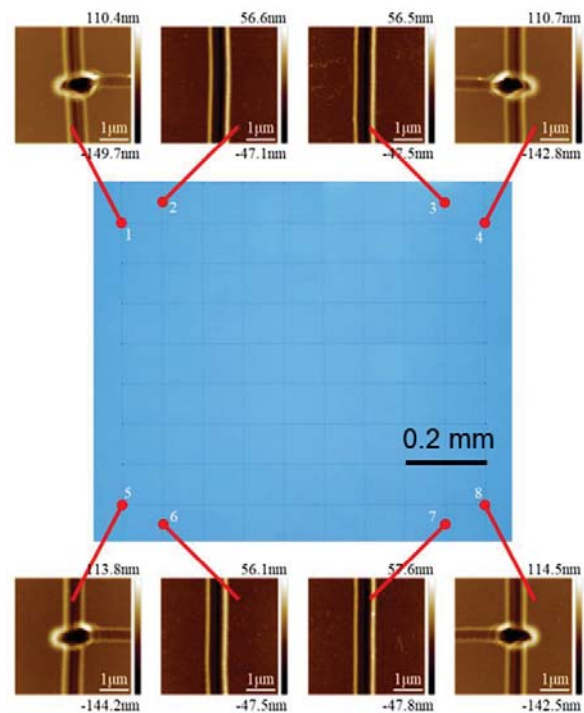


Fig. 6 Large-scale nano-grid structure.

4. Conclusions

In this study, a homemade micro/nano machining device is developed based on the contact mode of the AFM system. The hardware and software system of the device are developed. The output responses of the control system under sinusoidal wave signal with different frequencies are observed to verify the feasibility of variable force control machining. Nanoripple structures with controllable period are fabricated based on the variable force control method. Furthermore, a large-scale nano-grit is machined based on the proposed device.

ACKNOWLEDGEMENT

The authors gratefully acknowledge the financial supports of the Natural Science Foundation of China (52035004), Natural Science Foundation of Heilongjiang Province of China (YQ2020E015), Young Elite Scientist Sponsorship Program by CAST (No. YESS20200155), and the Fundamental Research Funds for the Central Universities (FRFCU5710050521, FRFCU5710091220).

REFERENCES

1. Yao, T., Wu, P., Wu, T., Cheng, C. and Yang, S., Fabrication of anti-reflective structures using hot embossing with a stainless steel template irradiated by femtosecond laser. *Microelectronic Engineering*, Vol. 88, pp. 2908-2912, 2011.
2. Wang, J., Yan, Y., Chang, S., Han, Y. and Geng, Y., Label-free surface-enhanced Raman spectroscopy detection of absorption manner of lysozyme based on nanodots arrays. *Applied Surface Science*, Vol. 509, pp. 145332, 2020.
3. Sun, M., Luo, C., Xu, L., Ji, H., Ouyang, Q., Yu, D., et al. Artificial Lotus Leaf by Nanocasting. *Langmuir*, Vol. 21, pp. 8978–8981, 2005.
4. Phan, H., Nguyen, T., Dinh, T., Iacopi, A., Hold, L., Shiddiky, M., et al., Robust Free - Standing Nano - Thin SiC Membranes Enable Direct Photolithography for MEMS Sensing Applications. *Adv Eng Mater*, Vol. 20, pp. 1700858, 2018.
5. Cho, Y., Park, J., Park, H., Cheng, X., Kim, B., Han, A., Fabrication of high-aspect-ratio polymer nanochannels using a novel Si nanoimprint mold and solvent-assisted sealing. *Microfluid Nanofluid*, Vol. 9, pp:163-70, 2010.
6. Wang, J., Yan, Y., Li, Z. and Geng, Y., Towards understanding the machining mechanism of the atomic force microscopy tip-based nanomilling process. *International Journal of Machine Tools and Manufacture*, Vol. 162, pp. 103701, 2021.